Effects of atomic short-range order on the electronic and optical properties of GaAsN, GaInN, and GaInAs alloys

L. Bellaiche and Alex Zunger
National Renewable Energy Laboratory, Golden, Colorado 80401
(Received 22 August 1997)

Using large ($\approx$500–1000 atoms) pseudopotential supercell calculations, we have investigated the effects of atomic short-range order (SRO) on the electronic and optical properties of dilute and concentrated GaAsN, GaInN, and GaInAs alloys. We find that in concentrated alloys the clustering of like atoms in the first neighbor fcc shell (e.g., N-N in GaAsN alloys) leads to a large decrease of both the band-gap and the valence-to-conduction dipole transition-matrix element in GaAsN and in GaInN. On the other hand, the optical properties of GaInAs depend only weakly on the atomic SRO. The reason that the nitride alloys are affected strongly by SRO while GaInAs is affected to a much lesser extent is that in the former case there are band-edge wave-function localizations around specific atoms in the concentrated random alloys. The property for such localization is already evident at the (dilute) isolated impurity and impurity-pair limits.
[S0163-1829(98)00507-4]

I. INTRODUCTION

GaN-based III-V semiconductors have recently attracted considerable attention due to their prospects in light-emitting device applications.[1,2] Theoretical studies have addressed optical properties relevant to such technological applications, including alloy band-gap bowing (see Refs. 3–6 and references therein). However, these theoretical studies have assumed perfect random alloys, while clustering (the embryonic stage of phase separation) and fully developed phase separation have been observed experimentally in GaAsN (Ref. 7) and GaInN alloys,[8–10] and are even thought to be responsible for the purple laser emission in GaInN.[9] Clustering in nitride alloys is, in fact, expected since nitrogen in GaAs and indium in GaN have limited solid solubilities due to the significant strain energies resulting from the large size mismatch between the solute and solvent atoms.[11] Although the equilibrium *surface* solubility can be up to five orders of magnitude larger than in the bulk,[12] away from the surface, the stabilizing surface effect diminishes, and the homogeneous alloy is no longer stable, and could cluster or phase separate. Thus, it is of interest to contrast the predicted optical properties of such alloys with and without local atomic clustering. Here, we will study theoretically the effect of short-range order (SRO) on the alloy strain energy, band-gap, transition matrix elements between the valence-band minimum (VBM) and the conduction-band maximum (CBM), and wave-function localization in $GaAs_{1-x}N_x$ and $Ga_{1-x}In_xN$ alloys. These alloys are representative of a broader class of nitride alloys: (a) The mixed-anion GaAsN alloy exhibits an As-impurity level inside the band gap at the As-dilute limit Ga<u>N</u>:As, and a nitrogen-localized CBM wave function at the opposite, nitrogen-dilute limit Ga<u>As</u>:N.[3] (b) The mixed-cation GaInN system exhibits a VBM wave-function localization around the indium impurity atom at the In-dilute limit <u>Ga</u>N:In, but no CBM localization exists at either impurity limits. To provide perspective, we will compare short-range order effects in these nitride alloys to those in a ''conventional'' III-V semiconductor alloy, namely, $Ga_{1-x}In_xAs$. This system has extended band-edge states, no gap level, and no wave-function localization at either dilute impurity limits. All of the alloys studied here exhibit direct band gap at all compositions.

We study two forms of short-range order: ''clustering,'' which implies association of *like atoms* (Ga-Ga and In-In in $Ga_{1-x}In_xN$) over what random statistics grants at that composition, and ''anticlustering,'' which implies association of *unlike atoms* (Ga-In in $Ga_{1-x}In_xN$) beyond random statistics. We will first briefly study ''impurity pairs'', e.g., two nitrogen in GaAs or two indium in GaN (see Sec. III) in order to better understand the effects of SRO in concentrated alloys (see Sec. IV).

Our main findings are the following. (i) In *dilute* alloys, strain energy *lowering* arrangements of the N-N pair in GaAs or In-In pair in GaN (e.g., when the two nitrogen atoms or the two indium atoms are second fcc neighbors) raise the band gap, while strain energy *increasing* configurations (e.g., first and fourth fcc neighbors N-N or In-In) lead to a *reduction* of the band gap. The change in band gap reflects the change in band-edge wave-function localization. (ii) In *concentrated* alloys, clustering of like atoms in the first neighbor fcc shell leads to (a) an increase in the strain energy, proportional to the lattice mismatch between the alloys bulk constituents, and (b) a large decrease of both the band-gap and the valence-to-conduction dipole transition matrix element in both GaAsN and GaInN. On the other hand, (c) the optical properties of GaInAs depend only weakly on the atomic SRO. The reason that the nitride alloys are affected strongly by SRO while GaInAs is affected to a much lesser extent is that in the former case there are band-edge wave-function localizations around specific atoms in the *concentrated random* alloys. The property for such localization is already evident at the dilute impurity limits.

II. METHODS

In studying clustering of *isolated impurity pairs* we will place two N atoms at different positions in GaAs, and two

 © 1998 The American Physical Society

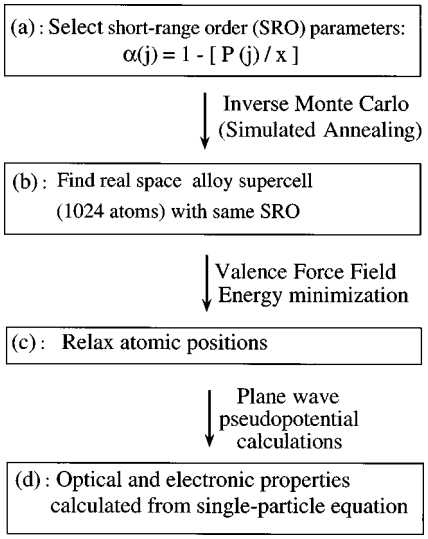

FIG. 1. Procedure used to simulate the effect of SRO on the structural, optical, and electronic properties in zinc-blende semiconductor alloys.

Ga atoms at different positions in InN. We will explore the effects of such ''elementary clusters'' on the strain energy, localization, and band gap. We explore impurity pairs that are first, second, third, and fourth fcc neighbors. The physical properties of the impurity pairs are compared with those of the random case, as mimic by the average over *all* the possible configurations of the pairs. Such pair geometries were studied in the past in the context of nitrogen pair spectra in GaP (Refs. 13–17) and in GaAs.[18] The atomic relaxations and the strain energy are predicted by the valence force field (VFF) approach[19,20] using the parameters of Ref. 21. The electronic structure is calculated via an empirical pseudopotential method[22] in a plane-wave basis. The screened pseudopotentials are fitted for bulk GaAs, GaN, InAs, and InN to *GW* band structures, experimental band gaps, and local-density approximation deformation potentials.[3] To calculate the near-gap eigensolutions of large supercells, we use the ''folded spectrum method,'' [23] which is a linear-in-size [''O(N)''] method, producing single-particle eigensolutions in a given energy window without having to obtain (and orthogonalize) to lower eigensolutions.

Our methodology for studying *concentrated* alloys is described in Fig. 1 and consists of four steps.

In the *first* step [Fig. 1(a)] we select a set of short-range order Cowley parameters

$$\alpha_j(x)=1-\frac{P(j)}{x}, \tag{1}$$

where $P(j)$ is the probability of finding a nitrogen (indium) atom being jth nearest-neighbor of an arsenic (gallium) atom in the mixed sublattice of the $GaAs_{1-x}N_x$ ($Ga_{1-x}In_xN$ and $Ga_{1-x}In_xAs$). $\alpha_j>0$ corresponds to an association of like atoms (e.g., clustering), while $\alpha_j<0$ corresponds to an association of unlike atoms (e.g., anticlustering). In the case of the perfect random alloys, $\alpha_j\equiv 0$ for all j's. For simplicity, we concentrate on the first fcc neighbor shell (e.g., Ga-In or Ga-Ga in $Ga_{1-x}In_xAs$) and we scan a range of α_1 values, keeping $\alpha_j\equiv 0$ for $j\neq 1$.

In the *second* step [Fig. 1(b)], we use an inverse Monte Carlo procedure (namely, a simulated annealing technique) to construct a large real-space supercell with occupation of lattice sites by Ga, and In in $Ga_{1-x}In_xAs$ so as to closely reproduce the SRO parameters selected in the first step. Good statistics are obtained using 1024 atoms per cell.

In the *third* step we relax the atomic positions inside the 1024 atoms supercells so as to minimize the VFF strain energy at each given $\{\alpha_j\}$ set [Fig. 1(c)]. As for the dilute cases, we use a conjugate gradient minimization of a parametrized valence force field. The strain energy resulting from relaxation is calculated from the same valence force field.

Once the relaxed atomic positions are determined, in the *final* step we calculate the electronic structure via the empirical pseudopotential method[22] in a plane-wave basis [Fig. 1(d)]. This gives us the band-gap and band-edge wave functions for each $\{\alpha_j\}$ set [Fig. 1(d)].

Once the near-gap energy states are known, we also calculate the momentum **P** matrix element:

$$M_{v,c}=|\langle\psi_v|\mathbf{p}|\psi_c\rangle|^2=\left|\sum_{\mathbf{G}}\mathbf{G}C_v^*(\mathbf{G})C_c(\mathbf{G})\right|^2, \tag{2}$$

where the sum runs over the vectors of the reciprocal space and where $C_v(\mathbf{G})$ and $C_c(\mathbf{G})$ are the coefficients of the plane-wave expansion of the alloy VBM state ψ_v and alloy CBM state ψ_c, respectively.

To understand the localization of the wave functions, it is useful to calculate the projection of the alloy wave function ψ_i on those of its zinc-blende virtual-crystal approximation (VCA) constituents $\phi_{n,\mathbf{k}}(\vec{r})$,

$$P_{i,n,\mathbf{k}}=|\langle\psi_i(\vec{r})|\phi_{n,\mathbf{k}}(\vec{r})\rangle|^2. \tag{3}$$

In the following, $P_{\mathrm{VBM}}(\Gamma)$ will denote the square of the projection of the alloy's valence-band maximum wave function on the Γ_{15v} VCA, while $P_{\mathrm{CBM}}(\Gamma)$ will denote the square of the projection of the conduction-band maximum wave function on the Γ_{1c} VCA state. As done in Ref. 24, we can use $P_{\mathrm{VBM}}(\Gamma)$ and $P_{\mathrm{CBM}}(\Gamma)$ to quantify the wave-function localization: a large value of these projections corresponds to an extended band-edge state, while a smaller value of these projections reflects localization in the real space.

A direct measure of the band-edge localization on particular atoms is given by the atomic-type parameter $Q_{\beta,i}$ (β = Ga, As, or N in $GaAs_{1-x}N_x$, and i = VBM or CBM) as

$$Q_{\beta,i}=\frac{F}{N_\beta}\frac{1}{[a(x)]^3}\sum_{j\epsilon\beta}\int_{V_j}|\psi_i|^2dV, \tag{4}$$

where the sum is over all the atomic sites j of type β. Here F is a normalization factor (equal to 27), N_β is the number of atoms of type β, $a(x)$ is the lattice constant of the alloy, and the integration of the square of the wave function ψ_i is performed in a volume $V_j=[a(x)/6]^3$ centered around atoms j of type β. The larger the value of $Q_{\beta,i}$, the larger is the localization of the ψ_i wave function on atoms of β type.

III. ISOLATED PAIRS

Figure 2 shows the calculated (i) strain energies (difference in total supercell elastic energy after and before substi-

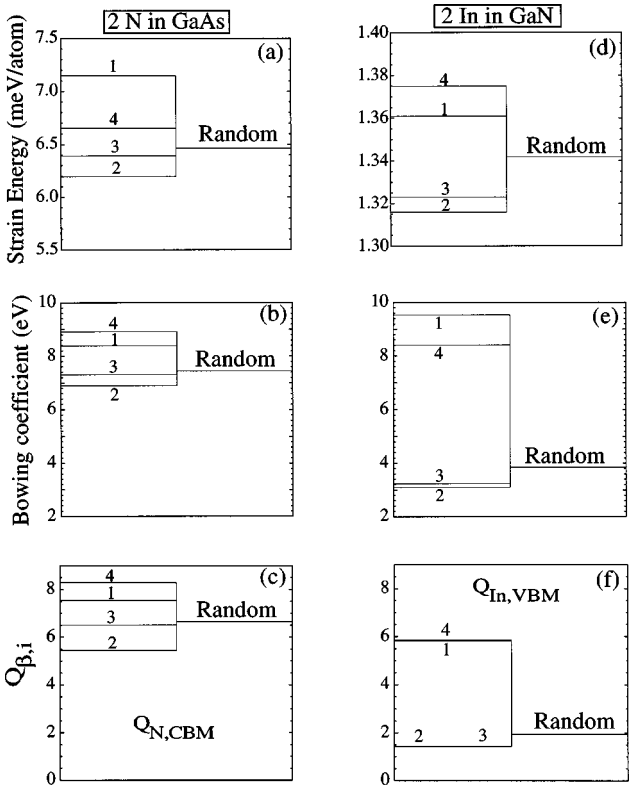

FIG. 2. Dependence of physical properties on the impurity pairs geometry. (a) and (d): Strain energy corresponding to nitrogen pairs in GaAs and to indium pairs in GaN, respectively. (b) and (e): Bowing coefficient corresponding to nitrogen pairs in GaAs and to indium pairs in GaN, respectively. (d): Conduction-band minimum localization parameter [see Eq. (4)] around nitrogen atoms for nitrogen pairs in GaAs. (f): Valence-band maximum localization parameter around indium atoms for indium pairs in GaN. The integers 1, 2, 3, and 4 denote the first, second, third, and fourth fcc neighbor positions of the mixed sublattice.

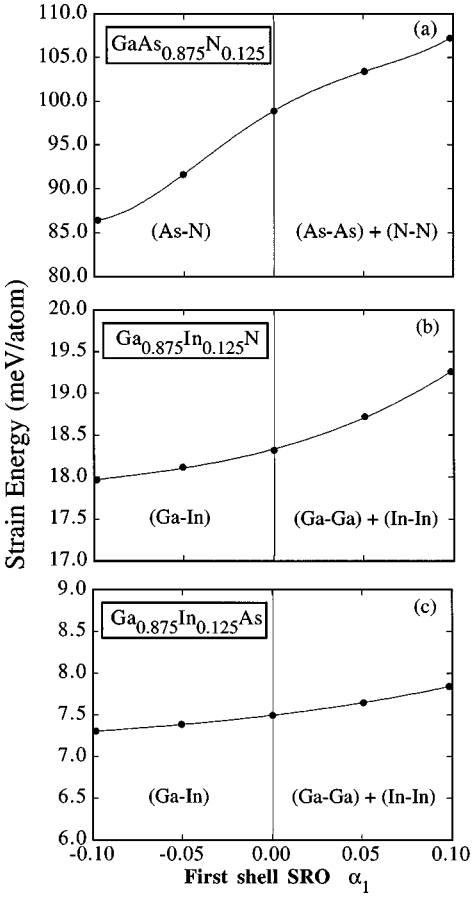

FIG. 3. Dependence of the strain energy on the SRO parameter α_1 of the first atomic shell in $GaAs_{0.875}N_{0.125}$ (a), $Ga_{0.875}In_{0.125}N$ (b), and $Ga_{0.875}In_{0.125}As$ (c). The parameters α_j, with $j \geqslant 2$, are set to their random values (i.e., zero). Note that the y scale of (a) is ten times larger than the y scale of (b) and (c). Inserts in parentheses indicate the type of SRO. In (a), for example, $\alpha_1 < 0$ means As-N association, while $\alpha_1 > 0$ means association of As-As and N-N.

tution of a pair of impurities), (ii) bowing coefficients of the direct band gap, and (iii) band-edge wave-function localization near the impurity atoms [cf. Eq. (4)], for N-N pairs in GaAs and In-In pairs in GaN. We have placed the two impurity atoms in a 512-atom supercell in four configurations, namely, first, second, third, and fourth fcc neighbor positions (denoted 1–4 in the figure). Parts (a) and (d) of Fig. 2 show that N-N and In-In prefer the second neighbor positions (largest lowering of strain energy), while the first neighbor N-N pair in GaAs, and the fourth neighbor In-In pair in GaN are energetically the least favorable. Figures 2(b) and 2(e) show that N-N clustering in GaAs, as well as In-In clustering in GaN leads to an increase in the band gap (reduction in bowing coefficient) with respect to the random alloy if the clustered impurities are placed in strain energy-minimizing positions (second and third neighbors). In contrast, if the impurities are placed in strain-energy raising positions (first and fourth neighbors), the band gap is considerably *reduced* (larger bowing coefficient) with respect to the random alloy: the difference in bowing coefficient can be as large as 1.5 eV for N-N pairs in GaAs and 5.5 eV for In-In pairs in GaN.

Previous theoretical studies[3,4] found that large wave-function localization leads to large bowing coefficient. We thus analyze the trends in the bowing coefficient in terms of wave-function localization: Figs. 2(c) and 2(f) show the quantity $Q_{\beta,i}$ [Eq. (4)] around the impurity atom β. We see that $Q_{\beta=N,i=\mathrm{CBM}}$ in GaAsN and $Q_{\beta=\mathrm{In},i=\mathrm{VBM}}$ in GaInN are both *reduced* (less localization) when the impurities are placed in strain energy lowering positions, while they are *increased* (more localization) when the impurities are placed in strain energy raising positions. On the other hand, we found that $Q_{\beta=\mathrm{N},i=\mathrm{VBM}}$ for N-N pairs in GaAs and $Q_{\beta=\mathrm{In},i=\mathrm{CBM}}$ for In-In pairs in GaN are insensitive to atomic arrangement. This dependence of band-edge state wave-function localization on SRO can be understood by considering the *single* impurity limits: in Ga<u>As</u>:N, the CBM exhibits localization around the nitrogen impurity while the VBM is preferentially localized around the majority atoms (arsenic).[3] Thus, the CBM of GaAs with nitrogen pairs is particularly sensitive to the mutual distance and to the symmetry of the nitrogen pair, while the VBM in the dilute alloys is quite insensitive to the nitrogen atomic arrangement. Similarly, we found that in <u>Ga</u>N:In, the VBM preferentially localizes around the indium impurity, while the CBM is extended. Thus, the VBM of In-In pairs in GaN is sensitive to the atomic arrangement of the impurity pairs, while the CBM does not respond to that.

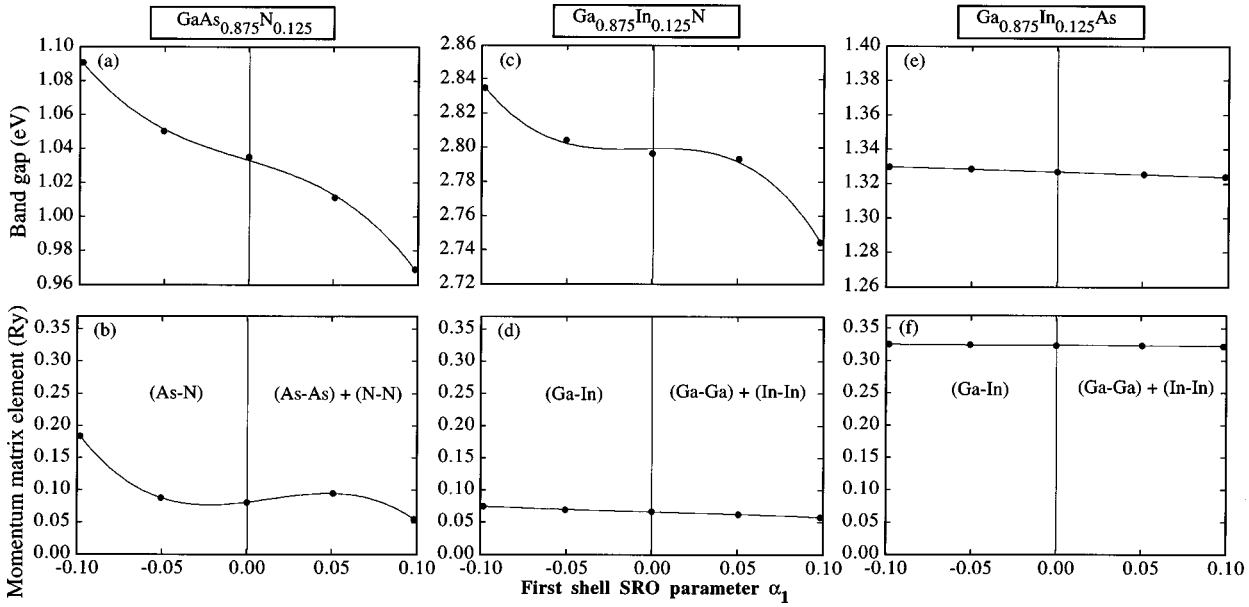

FIG. 4. Dependence of the band gap [(a), (c), and (e)] and of the transition dipole element [(b), (d), and (f)] on the SRO parameter α_1 of the first atomic shell in $GaAs_{0.875}N_{0.125}$ (left), $Ga_{0.875}In_{0.125}N$ (middle), and $Ga_{0.875}In_{0.125}As$ (right). The parameters α_j, with $j \geqslant 2$, are set to their random values (i.e., zero). Inserts in parentheses indicate the type of SRO. In (a), for example, $\alpha_1 < 0$ means As-N association, while $\alpha_1 > 0$ means association of As-As and N-N.

We also find that the band-edge states and the band gap of Ga-Ga pairs in InN, Ga-Ga pairs in InAs, and In-In pairs in GaAs depend only very slightly on the geometries of the pairs. This is consistent with the fact that we find no localization of the band-edge states at the dilute impurity limits InN:Ga, InAs:Ga, and GaAs:In. For example, the first neighbor Ga-Ga pair in InN leads to a slight increase of the bowing coefficient by less than 0.2 eV (from 1.14 to 1.31 eV) with respect to the random case. On the other hand, the energy of the highest occupied level and the degree of localization for an As-As pair in GaN are found to depend strongly on the pairs' geometry. This is consistent with the fact that GaN:As has a very deep As-impurity level above the valence-band maximum of GaN.[3] For example, the energy of the highest occupied level changes by more than 0.7 eV when the As-As pair changes from being first to second fcc neighbor in GaN.

IV. CONCENTRATED ALLOYS

We chose to focus on an impurity composition $x = 0.125$ because of its relevance to experiment: Bi and Tu (Ref. 25) grew GaAsN alloys up to 13–14% of nitrogen, and the active region of blue-purple laser emission from GaInN alloys have an average indium composition close to 12.5%.[9]

A. Strain energies associated with SRO

Figure 3 shows the dependence of the strain energy on the first-shell SRO parameter α_1 for the three alloys studied. Two interesting features emerge: (i) The strain energy increases with α_1. This appears to be a universal characteristic of zinc-blende semiconductor alloy as noted in previous calculations.[26–28] It implies that at equilibrium, these alloys will adopt anticlustering (e.g., $\alpha_1 < 0$). This is consistent with recent experimental observations of anticlustering for the first fcc neighbor shell in GaInAs alloys.[29] Note, however, that most nitride alloys appear to be grown out of equilibrium as evidenced by the incorporation of nitrogen in GaAs far above the equilibrium solubility limit.[30] In fact, clustering, rather than anticlustering, is observed.[7–10]

(ii) The increase in strain energy with α_1 is proportional to the lattice mismatch of the bulk constituents of the alloys: the difference in strain energy in the 20% lattice mismatch $GaAs_{0.875}N_{0.125}$ is equal to 20 meV/atom when going from $\alpha_1 = -0.10$ to 0.10 [Fig. 3(a)], while the same variation of α_1 produces an increase of only 1.3 and 0.5 meV/atom in the 10% lattice mismatch $Ga_{0.875}In_{0.125}N$ [Fig. 3(b)] and in the 7% lattice mismatch $Ga_{0.875}In_{0.125}As$ [Fig. 3(c)], respectively.

B. Band gaps and transition matrix elements

Figure 4 shows the dependence of the band gap and the dipole transition matrix element on the first shell SRO parameter. We see that anticlustering (e.g., $\alpha_1 < 0$) in zinc-blende semiconductor alloys leads to an increase in both the direct band-gap and the momentum matrix element with respect to the random case ($\alpha_j \equiv 0$), while clustering decreases the band-gap and the momentum matrix element (i.e., the photoluminescence intensity). This is consistent with the calculations[31] predicting that a large positive value of α_1 (around $+0.17$) in $Al_{0.5}Ga_{0.5}As$, $Al_{0.5}In_{0.5}As$, and $Ga_{0.5}In_{0.5}P$ decreases the direct band gap with respect to that of the random alloys. It can also be seen from Fig. 4 that the effects of SRO are larger for the nitride alloys than for the conventional GaInAs alloy. For example, the difference in band gap in $Ga_{0.875}In_{0.125}As$ as α_1 changes from -0.10 to $+0.10$ is only 6 meV (corresponding to a variation of 0.45% with respect to the band gap of the random alloys and leading to small change in the bowing coefficient from 0.48 to 0.53 eV) [Fig. 4(e)], while the same variation of α_1 in $GaAs_{0.875}N_{0.125}$

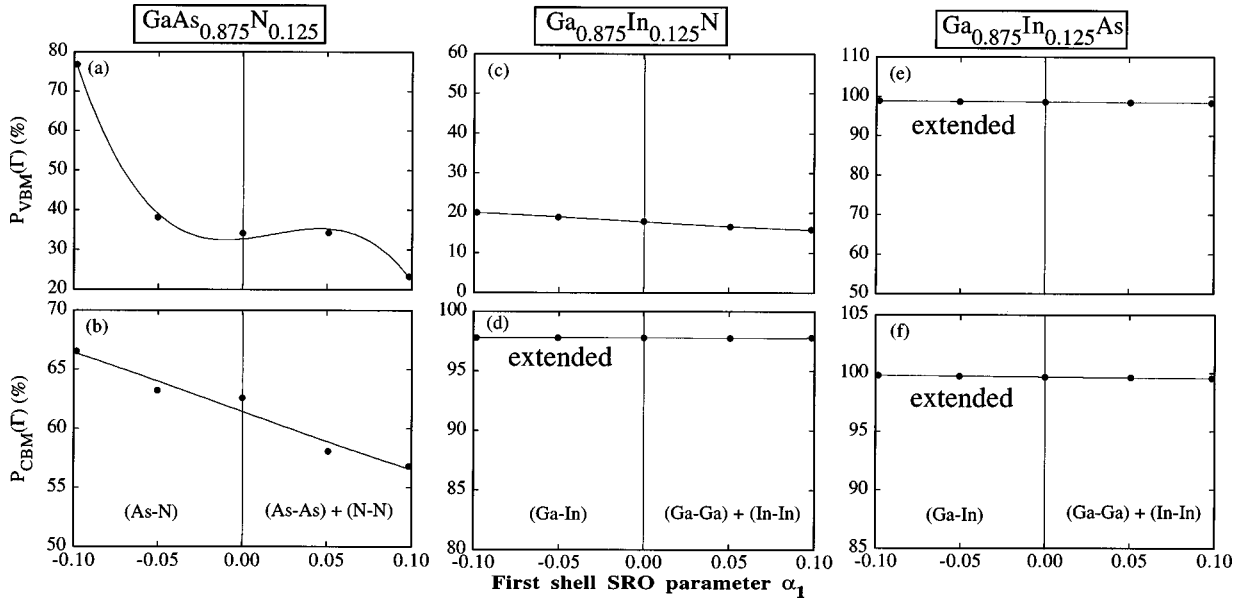

FIG. 5. Dependence of the VBM localization [(a), (c), and (e)] and of the CBM localization [(b), (d), and (f)] on the SRO parameter α_1 of the first atomic shell in $GaAs_{0.875}N_{0.125}$ (left), $Ga_{0.875}In_{0.125}N$ (middle), and $Ga_{0.875}In_{0.125}As$ (right). The parameters α_j, with $j \geqslant 2$, are set to their random values (i.e., zero). Inserts in parentheses indicate the type of SRO. In (a), for example, $\alpha_1 < 0$ means As-N association, while $\alpha_1 > 0$ means association of As-As and N-N.

produces a decrease of the band gap of 122 meV [Fig. 4(a)] (corresponding to a variation of 12% with respect to the band gap of the random alloy and leading to a change in the bowing coefficient from 5.9 to 7.0 eV). The corresponding difference in band gap in $Ga_{0.875}In_{0.125}N$ alloys is 90 meV, corresponding to a variation of 3% with respect to the band gap of the random alloy and leading to a change in optical bowing coefficient from 2.4 to 3.2 eV. These bowing coefficients are larger than the previous theoretical result of 1 eV found for the random zinc-blende $Ga_{0.50}In_{0.50}N$ alloy.[5] As a matter of fact, a bowing coefficient much larger than 1 eV has been indeed observed experimentally in $Ga_{1-x}In_xN$ alloys, for indium compositions lower than 20%.[32–34] The large sensitivity of nitride alloys to SRO suggests that experimental investigations of the generic effects of short-range order on material properties (which are very frequent in metallic alloys[35] but scant in semiconductor alloys; see recent review in Ref. 36) are best undertaken on nitride alloys. Indeed, this large sensitivity of the band gap to SRO has been observed experimentally in GaInN alloys: the formation of indium-rich clusters in $Ga_{1-x}In_xN$ alloys with $x \equiv 10-20\%$ leads to a decrease of the band gap by 170–250 meV with respect to the band gap of the random alloy.[9] The existence of SRO may also explain the different values found experimentally for the band gap of $GaAs_{1-x}N_x$ alloys having the same nominal nitrogen composition but grown under different conditions.[37,38]

C. The band-edge wave-function localizations

Mader and Zunger[31] showed that large clustering in GaAlAs and GaInP alloys leads to a decrease of the direct band gap accompanied by an enhancement of band-edge wave-function localizations. In line with that, we analyze the trends of the optical properties with SRO in terms of wave-function localization: Fig. 5 shows $P_{\mathrm{VBM}}(\Gamma)$ and $P_{\mathrm{CBM}}(\Gamma)$ [Eq. (3)] in the three alloys studied here. It demonstrates that indeed the behavior of the band-gap and the momentum matrix element are correlated with band-edge wave-function localizations: As α_1 increases, the VBM and CBM wave functions of $GaAs_{0.875}N_{0.125}$ alloys localize more [e.g., $P_{\mathrm{VBM}}(\Gamma)$ and $P_{\mathrm{CBM}}(\Gamma)$ decrease], while, at the same time, the band gap and the momentum matrix element both decrease [Figs. 4(a) and 4(b)]. By calculating the atom-resolved localization parameter $Q_{\beta,i}$ [Eq. (4)], we can find where the localization occurs. Figure 6(a) shows that the localization of the CBM is strongest around the nitrogen atoms. Similarly, we found that the localization of the VBM is strongest around the arsenic atoms.[3]

In contrast to the case of $GaAs_{0.875}N_{0.125}$, Figs. 5(e) and 5(f) indicate that the band-edge states of $Ga_{0.875}In_{0.125}As$ alloys are extended and so do not depend on the SRO α_1 parameter. This is evident by the fact that $P_{\mathrm{VBM}}(\Gamma)$ and $P_{\mathrm{CBM}}(\Gamma)$ are large (around 99%) and independent of α_1, and by the fact that the real-space localization parameters for the CBM of $Ga_{0.875}In_{0.125}As$ are only weakly dependent on the SRO [cf. Fig. 6(a)]. This extended nature of the GaInAs band-edge states thus implies the insensitivity of both the band gap and the momentum matrix element with SRO [Figs. 4(e) and 4(f)].

The situation of $Ga_{0.875}In_{0.125}N$ is intermediate between that of $GaAs_{0.875}N_{0.125}$ and $Ga_{0.875}In_{0.125}As$, in the sense that only one band-edge state depends on the SRO: clustering in $Ga_{0.875}In_{0.125}N$ leads to a larger localization of the VBM [$P_{\mathrm{VBM}}(\Gamma)$ decreases by 25% when α_1 ranges from -0.10 to $+0.10$, cf. Fig. 5(c)], while the CBM is an extended state that does not respond to the local atomic arrangement [$P_{\mathrm{CBM}}(\Gamma)$ is around 98% and is independent of α_1 (Fig. 5)]. We found that the localization of the VBM in $Ga_{0.875}In_{0.125}N$ occurs both around the indium atoms and around the nitrogen atoms surrounded by indium atoms. This VBM localiza-

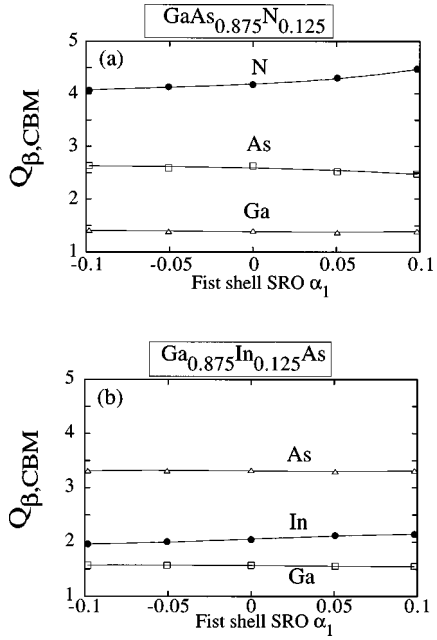

FIG. 6. Dependence of the localization parameter $Q_{\beta,i}$ of atoms of type β=As, N, Ga, or In [Eq. (4)] for the i=CBM state on the first atomic shell in $GaAs_{0.875}N_{0.125}$ (a) and $Ga_{0.875}In_{0.125}As$ (b).

tion is consistent with the decrease of the band gap and the decrease of the momentum matrix element as α_1 increases [Figs. 4(c) and 4(d)]. For example, since Ref. 24 demonstrated that the momentum matrix element is directly proportional to the product $P_{\mathrm{VBM}}(\Gamma)\times P_{\mathrm{CBM}}(\Gamma)$, and since Fig. 5(d) shows that in GaInN alloys $P_{\mathrm{CBM}}(\Gamma)$ is independent of α_1, we can conclude that there is a one-by-one correspondence between the 25% decrease of the momentum matrix element [cf. Fig. 4(d)] and the 25% decrease of $P_{\mathrm{VBM}}(\Gamma)$ when α_1 ranges from -0.10 to $+0.10$ [cf. Fig. 5(c)].

Our foregoing discussion shows that the only states insensitive to the SRO are the states which are extended in the random alloys, i.e., for which $P_{i,n,\mathbf{k}}$ (i=VBM or CBM and $\mathbf{k}=\mathbf{0}$) are larger than 95% for $\alpha_j\equiv 0$. The nature (extended or localized) of the band-edge wave functions in the *random* alloys can be understood by considering the dilute limits. In GaAs:N, the CBM exhibits localization around the nitrogen impurity.[3] This continues to be so in the As-rich alloy where the CBM localizes preferentially around the nitrogen atoms.[3] Thus, the energy of the CBM is particularly sensitive to the nitrogen atomic arrangement. On the other hand, the VBM of this anion-mixed nitride alloy localizes strongly around arsenic atoms[3] [since GaN:As exhibits an As-impurity gap level located above the VBM of GaN (Ref. 3)]. Thus, the energy of the VBM is particularly sensitive to the arsenic atom arrangement.

Similarly, the VBM of $Ga_{0.875}In_{0.125}N$ is also sensitive to the SRO, since in GaN:In, the VBM preferentially localizes around the indium impurity and around the nitrogen atoms first neighbors of this indium. In the same manner, the insensitivity of the CBM of $Ga_{0.875}In_{0.125}N$ and of both the VBM and CBM of $Ga_{0.875}In_{0.125}As$ to SRO can be understood by noticing that there is no localization of these band-edge states at the corresponding single impurity limits.

We have thus observed that any state exhibiting wavefunction localization at the dilute impurity limit is sensitive to the local atomic arrangement in the concentrated alloys and in the impurity pairs case (Fig. 2 and Sec. III).

V. SUMMARY

We investigated the effects of the atomic first shell SRO parameter in concentrated GaAsN, GaInN, and GaInAs alloys. We found the following. (i) Clustering leads to an increase of the strain energy. The magnitude of this increase is proportional to the lattice mismatch of the alloys: this increase is larger for GaAsN (lattice mismatch around 20%) than for GaInN (lattice mismatch around 10%) and for GaInAs (lattice mismatch around 7%). (ii) Clustering leads to a large decrease of the band gap and to a consequent decrease of the momentum matrix element in both GaAsN and in GaInN, while the optical properties of GaInAs only slightly depend on the atomic arrangement. The differences of behavior of the band gap and of the momentum matrix element with SRO in nitride alloys with respect to the conventional GaInAs alloys are driven by band-edge wavefunction localizations occurring around specific atoms in nitride alloys. This localization is evident already at the dilute and pairs impurity limits.

ACKNOWLEDGMENTS

We wish to thank C. Wolverton, L. W. Wang, S-H. Wei, and K. Mader for useful discussions. This work was supported by the U.S. Department of Energy, OER-BES-DMS Grant No. DE-AC36-83-CH10093.

[1] S. Nakamura, Adv. Mater. **8**, 689 (1996).
[2] T. Matsuoka, Adv. Mater. **8**, 469 (1996).
[3] L. Bellaiche, S.-H. Wei, and A. Zunger, Phys. Rev. B **54**, 17 568 (1996).
[4] S.-H. Wei and A. Zunger, Phys. Rev. Lett. **76**, 664 (1996).
[5] A. F. Wright and J. S. Nelson, Appl. Phys. Lett. **66**, 3051 (1995).
[6] W. R. L. Lambrecht, Solid-State Electron. **41**, 195 (1997).
[7] R. S. Goldman, R. M. Feenstra, B. G. Briner, M. L. O'Steen, and R. J. Hauenstein, Appl. Phys. Lett. **69**, 3698 (1996).
[8] K. Osamura, S. Naka, and Y. Murakami, J. Appl. Phys. **46**, 3432 (1975).
[9] Y. Narakawa, Y. Kawakami, M. Funato, S. Fujita, S. Fujita, and S. Nakamura, Appl. Phys. Lett. **70**, 981 (1997).
[10] R. Singh, D. Doppalapudi, T. D. Moustakas, and L. I. Romano, Appl. Phys. Lett. **70**, 1089 (1997).
[11] I. Ho and G. B. Stringfellow, Appl. Phys. Lett. **69**, 2701 (1996).
[12] S. B. Zhang and A. Zunger, Appl. Phys. Lett. **71**, 677 (1997).
[13] E. Cohen and M. D. Sturge, Phys. Rev. B **15**, 1309 (1977).
[14] R. A. Faulkner, Phys. Rev. **175**, 991 (1968).
[15] S. Brand and M. Jaros, J. Phys. C **72**, 525 (1979).
[16] M.-F. Li, D.-Q. Mao, and S.-Y. Ren, Phys. Rev. B **32**, 6907 (1985).

[17] B. Gil, Physica B & C **146**, 84 (1987).
[18] X. Liu, M.-E. Pistol, L. Samuelson, S. Schwetlick, and W. Seifert, Appl. Phys. Lett. **56**, 1451 (1990).
[19] P. N. Keating, Phys. Rev. **145**, 637 (1966).
[20] R. M. Martin, Phys. Rev. B **1**, 4005 (1970).
[21] K. Kim, W. R. L. Lambrecht, and B. Segall, Phys. Rev. B **53**, 16 310 (1996).
[22] K. Mader and A. Zunger, Phys. Rev. B **50**, 17 393 (1994).
[23] L.-W. Wang and A. Zunger, J. Chem. Phys. **100**, 2394 (1994).
[24] L. Bellaiche, S.-H. Wei, and A. Zunger, Phys. Rev. B **56**, 10 233 (1997).
[25] W. G. Bi and C. W. Tu, Appl. Phys. Lett. **70**, 1608 (1997).
[26] A. Silverman, A. Zunger, R. Kalish, and J. Adler, Phys. Rev. B **51**, 10 795 (1995); Europhys. Lett. **31**, 373 (1995).
[27] C. Wolverton and A. Zunger, Phys. Rev. Lett. **75**, 3162 (1995).
[28] S.-H. Wei, L. G. Ferreira, and A. Zunger, Phys. Rev. B **41**, 8240 (1990).
[29] K. J. Chao, C. K. Shih, D. W. Gotthold, and B. G. Streetman, (unpublished).
[30] Y. Qiu, S. A. Nikishin, H. Temkin, V. A. Elyukhin, and A. Kudriavstev, Appl. Phys. Lett. **70**, 2831 (1997).
[31] K. Mader and A. Zunger, Phys. Rev. B **51**, 10 462 (1995).
[32] N. Yoshimoto, T. Matsuoka, T. Sasaki, and A. Katsui, Appl. Phys. Lett. **57**, 1031 (1990).
[33] W. Li, P. Bergman, I. Ivanov, W.-X. Ni, H. Amano, and I. Akasa, Appl. Phys. Lett. **69**, 3390 (1996).
[34] T. Takeuchi, H. Takeuchi, S. Sota, H. Sakai, H. Amano, and A. Akasaki, Jpn. J. Appl. Phys., Part 2 **36**, L177 (1997).
[35] L. Reinhard and S. C. Moss, Ultramicroscopy **52**, 223 (1993).
[36] A. Zunger and S. Mahajan, in *Handbook on Semiconductors*, 2nd ed., edited by T. S. Moss and S. Mahajan (Elsevier, Amsterdam, 1994), Vol. 3, pp. 1399–1513.
[37] A. Ougazzaden, Y. Le Bellego, E. V. K. Rao, M. Juhel, L. Leprince, and G. Patriarche, Appl. Phys. Lett. **70**, 2861 (1997).
[38] S. Francoeur (private communication).